# Silver(I)/Bipyrazole/Dicarboxylate Interpenetrated Coordination Networks: Spontaneous Chiral Resolution, Modulation of Topologies, Water Clusters, and Photoluminescences

**ARTICLE** *in* CRYSTAL GROWTH & DESIGN · APRIL 2014

Impact Factor: 4.89 · DOI: 10.1021/cg401805x

CRYSTAL GROWTH & DESIGN

Article

pubs.acs.org/crystal

# Silver(I)/Bipyrazole/Dicarboxylate Interpenetrated Coordination Networks: Spontaneous Chiral Resolution, Modulation of Topologies, Water Clusters, and Photoluminescences

Lu-Lu Han,[†] Xi-Ying Zhang,[‡] Jiang-Shan Chen,[†] Zhong-Hui Li,[†] Dao-Feng Sun,*[,§] Xing-Po Wang,[†] and Di Sun*[,†]

[†]Key Lab for Colloid and Interface Chemistry of Education Ministry, School of Chemistry and Chemical Engineering, Shandong University, Jinan, 250100, People's Republic of China

[‡]State Key Laboratory of Crystal Materials, Shandong University, Jinan, 250100, People's Republic of China

[§]College of Science, China University of Petroleum (East China), Qingdao, Shandong 266580, People's Republic of China

Supporting Information

**ABSTRACT:** Seven novel silver(I) coordination networks with mixed flexible 3,3′,5,5′-tetramethyl-4,4′-bipyrazole (bpz) and C3−C9 aliphatic dicarboxylic acids, $[Ag_2(bpz)_4(mal)\cdot 7H_2O]_n$ (**1***L* and **1***R*), $[Ag_2(bpz)_3(suc)]_n$ (**2**), $[Ag_4(bpz)_5(glu)_2]_n$ (**3**), $[Ag_4(bpz)_5(adip)_2]_n$ (**4**), $[Ag_4(bpz)_7(pim)_2\cdot 12H_2O]_n$ (**5**), $[Ag_2(bpz)_4(sub)\cdot 7H_2O]_n$ (**6**), and $[Ag_2(bpz)_3(aze)\cdot 3.5H_2O]_n$ (**7**) ($H_2$mal = malonic acid, $H_2$suc = succinic acid, $H_2$glu = glutaric acid, $H_2$adip = adipic acid, $H_2$pim = pimelic acid, $H_2$sub = suberic acid, $H_2$aze = azelaic acid), have been synthesized and structurally characterized by single-crystal X-ray diffraction analyses and further characterized by infrared spectra (IR), elemental analyses, powder X-ray diffraction (PXRD), and thermogravimetric analyses (TGA). Single crystal X-ray diffraction analysis reveals that **1** crystallized into a pair of enantiomerically pure 3D 3-fold interpenetrated chiral $SrSi_2$ networks (point symbol $\{10^3\}$) through spontaneous resolution in the absence of any chiral source. Complex **2** is a 3D 2-fold interpenetrated 3-connected uninodal **dia-f** network (point symbol $\{4\cdot 14^2\}$) without consideration of Ag···Ag interaction. Complexes **3** and **4** are similar 2D + 2D → 2D $6^3$-**hcb** layer featuring 3-fold parallel interpenetration. Complex **5** is a 3D 3-fold interpenetrated 3,4-connected **3,4T1** network (point symbol $\{4\cdot 6\cdot 8\}\{4\cdot 6^2\cdot 8^3\}$). Complexes **6** and **7** are similar 2D + 2D → 2D **fes** layers (point symbol $\{4\cdot 8^2\}$) featuring 3-fold parallel interpenetration. In **1**−**7**, structural diversity ranging from 2D **hcb** and **fes** layers to 3D chiral $SrSi_2$, achiral **dia-f**, and **3,4T1** networks is modulated by dicarboxylates with alkyl chains of different lengths. Interestingly, a well-resolved octanuclear water cluster built from a chairlike $(H_2O)_6$ cluster and two water molecules dangling on two corners of it and a unusual seesaw-like pentanuclear water cluster is observed in the voids of **5** and **7**, respectively. Furthermore, the solid-state photoluminescence properties of the **1**−**7** were investigated at 298 and 77 K.

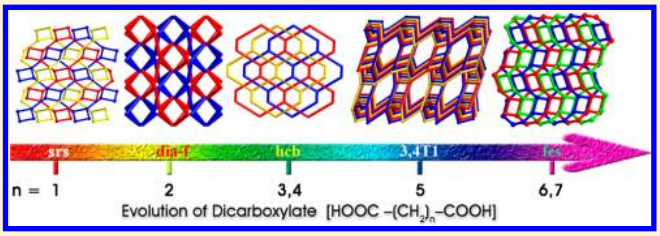


## INTRODUCTION

Over the past decades, much interest has been witnessed in creating a variety of coordination compounds, especially those with various entangled features, due to their aesthetic appeal of molecular connectivities and topologies, as well as the potential applications in luminescence, magnetism, sensors, gas adsorption, ion exchange, conductivity, and catalysis.[1,2] Since many factors including coordination requirements of central metal and the features of organic ligand, solvent, temperature, ratio of reactants, reaction time, pH, and so on[3] could influence the self-assembly results, it is still a huge challenge to design and predict a new coordination networks with a specific net topology.[4] Currently, experiment−feedback−experiment exploration mode still dominates the field of crystal engineering and incessantly enriches and deepens our comprehension on coordination-driven self-assembly. In this process, an effective and controllable route is to systematically change one of influence factors and then seek out how these changes influence the resultant structures and even their properties. Until now, most new finds in the crystal engineering field are still based on random change of more than one of the above-mentioned factors, which surely produces different structures but hardly gives wide audiences definitive information on self-assembly, so systematical investigations are urgent in this field.

As we know, the nature of the ligand significantly contributes to the final network structure. The 3,3′,5,5′-tetramethyl-4,4′-bipyrazole (bpz) ligand possesses considerable flexibility introduced by the free rotation of two pyrazolyl rings around the central C−C bond with wide interplanar angles of 50−90°,[5] which could then adjust the distances between two bridged metal centers. As a result, bpz has a variable bridging orientation and can diversify the dimensionalities and top-

Received: December 4, 2013
Revised: March 17, 2014

   dx.doi.org/10.1021/cg401805x | Cryst. Growth Des. XXXX, XXX, XXX−XXX

ologies of coordination networks. The soft acid Ag(I) ion possesses a wide range of coordinative numbers from two to six, even seven and eight, and demonstrates a strong tendency to display Ag(I)···Ag(I) interactions.[6] Thus, the Ag(I) ion can serve as an excellent candidate to link bridging ligands and form polymeric networks with novel coordination patterns.[7]

To survey the influence of length of the bridging ligands used, it is important to have a system devoid of small inorganic or organic counteranions, since counteranions also play a prominent role in shaping the resultant architectures. This can be achieved by combining metal ions with a mixed neutral N ligand and anionic dicarboxylate ligands that result in MOFs with intriguing topologies and functional properties, where the assembly process is more controllable than in a single ligand system.[8,9] As indicated by a CSD (Cambridge Structure Database) survey with the help of ConQuest, version 1.3,[10] there are only 20 silver(I)/bipyrazole coordination networks[11] containing 7 Ag(I)/bpz complexes incorporating different anions, such as $NO_3^-$, $PO_2F_2^-$, $ClO_4^-$, $CF_3SO_3^-$, $CH_3CO_2^-$, $CF_3CO_2^-$, $CF_3CF_2CO_2^-$, and $H_2PO_4^-$, and only 2 Ag(I)/bpz/aromatic dicarboxylate complexes, but no systematic study of the effect of chain length of the aliphatic dicarboxylate on the Ag(I)/bpz system has been carried out. The possible reason is the flexibility of aliphatic dicarboxylates, which hampers the formation of crystalline complexes. Therefore, the construction of diverse coordination networks from Ag(I), bpz, and the aliphatic dicarboxylates is a challenging and interesting project.

With these concepts in mind and our previous work,[12] we hydrothermally assembled $Ag_2O$, bpz, and dicarboxylates with varied carbon chain length of one to seven (Scheme 1), giving

**Scheme 1. Structures of N- and O-Donor Ligands Used in This Work**

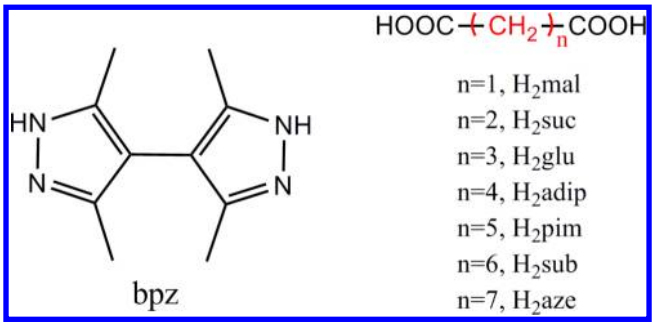


seven novel silver(I)/bipyrazole/dicarboxylate coordination networks, namely, $[Ag_2(bpz)_4(mal)\cdot 8H_2O]_n$ (**1*L*** and **1*R***), $[Ag_2(bpz)_3(suc)]_n$ (**2**), $[Ag_4(bpz)_5(glu)_2]_n$ (**3**), $[Ag_4(bpz)_5(adip)_2]_n$ (**4**), $[Ag_4(bpz)_7(pim)_2\cdot 12H_2O]_n$ (**5**), $[Ag_2(bpz)_4(sub)\cdot 7H_2O]_n$ (**6**), and $[Ag_2(bpz)_3(aze)\cdot 4H_2O]_n$ (**7**) ($H_2$mal = malonic acid, $H_2$suc = succinic acid, $H_2$glu = glutaric acid, $H_2$adip = adipic acid, $H_2$pim = pimelic acid, $H_2$sub = suberic acid, $H_2$aze = azelaic acid), which range from 2D **hcb** and **fes** layers to 3D chiral $SrSi_2$, achiral **dia-*f***, and **3,4T1** networks. The spontaneous chiral resolution in **1**, novel water clusters in **5** and **7**, and luminescent properties of **1**–**7** are also investigated.

## EXPERIMENTAL SECTION

**Materials and General Methods.** All chemicals and solvents used in the syntheses were of analytical grade and used without further purification. C, N, and H analyses were performed on an EA1110 CHNS-0 CE 65 elemental analyzer. IR (KBr pellet) spectra were recorded on a Nicolet Magna750FT-IR spectrometer. Powder-XRD measurements were recorded on a D/Max-2500 X-ray diffractometer using Cu K$\alpha$ radiation. Photoluminescence spectra were measured on a Hitachi F-7000 fluorescence spectrophotometer equipped with Dewar flask with a Suprasil quartz coldfinger. Thermogravimetric analyses (TGA) were performed on a Netzsch STA 449C thermal analyzer from room temperature to 800 °C under nitrogen atmosphere at a heating rate of 10 °C/min. UV–vis measurements (diffuse-reflectance mode) were carried on a Varian Cary5000 UV–vis–NIR spectrophotometer equipped with an integrating sphere at 298 K. The pH values were measured on a pHs-3C (08) digital pH-meter (REX, Shanghai, China).

**Preparation of Complexes 1–7.** *$[Ag_2(bpz)_4(mal)\cdot 7H_2O]_n$ (**1*L*** and **1*R***).* A mixture of $Ag_2O$ (23.2 mg, 0.1 mmol), bpz (38 mg, 0.2 mmol), $H_2$mal (20.8 mg, 0.2 mmol), 6 mL of $H_2O$, and 0.15 mL of pyridine was heated to 120 °C in 8 h in a 25 mL Teflon-lined reaction vessel, kept at 120 °C for 33 h, and then slowly cooled to 30 °C in 13 h. The pH values of the system are 5.75 and 6.03 before and after the solvothermal reaction. Colorless needle-like crystals of **1** was isolated by filtration, washed with $H_2O$, and dried in air (yield: 38% based on bpz). Elemental analysis calcd (%) for **1** ($C_{43}H_{72}Ag_2N_{16}O_{11}$) C 42.86, H 6.02, N 18.60; found C 42.29, H 6.75, N 18.45. Selected IR peaks ($cm^{-1}$): 3201(s), 3078(m), 1573(s), 1415(m), 1309(w), 1255(w), 1168(w), 1015(s), 783(m).

*$[Ag_2(bpz)_3(suc)]_n$ (**2**).* A mixture of $Ag_2O$ (23.2 mg, 0.1 mmol), bpz (38 mg, 0.2 mmol), $H_2$suc (23.6 mg, 0.2 mmol), and 6 mL of $H_2O$ was heated to 180 °C in 10 h in a 25 mL Teflon-lined reaction vessel, kept 180 °C for 50 h, and then slowly cooled to 30 °C in 13 h. The pH values of system are 3.59 and 3.60 before and after the solvothermal reaction. Colorless needle-like crystals of **2** were isolated by filtration, washed with $H_2O$, and dried in air (yield 41% based on bpz). Elemental analysis calcd (%) for **2** ($C_{17}H_{23}AgN_6O_2$) C 45.25, H 5.14, N 18.62; found C 45.79, H 5.65, N 18.42. Selected IR peaks ($cm^{-1}$): 3163(m), 2923(m), 1577(s), 1417(s), 1296(m), 1214(w), 1164(w), 1018(m), 872(w), 781(w), 650(w), 524(w).

*$[Ag_4(bpz)_5(glu)_2]_n$ (**3**).* Synthesis of complex **3** was similar to that of **2** but using $H_2$glu (26.4 mg, 0.2 mmol) instead of $H_2$suc (23.6 mg, 0.2 mmol). The pH values of system are 3.72 and 3.63 before and after the solvothermal reaction. Colorless needle-like crystals of **3** were isolated by filtration, washed with $H_2O$, and dried in air (yield 57% based on bpz). Elemental analysis calcd (%) for **3** ($C_{30}H_{41}Ag_2N_{10}O_4$) C 43.86, H 5.03, N 17.05; found C 43.16, H 5.33, N 16.89. Selected IR peaks ($cm^{-1}$): 3201(m), 1564(s), 1405(m), 1309(w), 1168(w), 1015(m), 779(w).

*$[Ag_4(bpz)_5(adip)_2]_n$ (**4**).* Synthesis of complex **4** was similar to that of **2** but using $H_2$adip (29.2 mg, 0.2 mmol) instead of $H_2$suc (23.6 mg, 0.2 mmol). The pH values of system are 3.73 and 3.88 before and after the solvothermal reaction. Colorless needle-like crystals of **4** were isolated by filtration, washed with $H_2O$, and dried in air (yield 49% based on bpz). Elemental analysis calcd (%, for $C_{31}H_{43}Ag_2N_{10}O_4$) C 44.57, H 5.19, N 16.77; found C 44.28, H 5.32, N 16.92. Selected IR peaks ($cm^{-1}$): 3200(w), 2928(w), 1566(s), 1405(m), 1310(w), 1177(w), 1019(w), 772(w).

*$[Ag_4(bpz)_7(pim)_2\cdot 12H_2O]_n$ (**5**).* A mixture of $Ag_2O$ (11.6 mg, 0.05 mmol), bpz (19 mg, 0.1 mmol), $H_2$pim (16 mg, 0.1 mmol), and 6 mL of $H_2O$ was heated to 120 °C in 10 h in a 25 mL Teflon-lined reaction vessel, kept 120 °C for 33 h, and then slowly cooled to 30 °C in 13 h. The pH values of system are 3.90 and 3.98 before and after the solvothermal reaction. Colorless needlelike crystals of **5** were isolated by filtration, washed with $H_2O$, and dried in air (yield 62% based on bpz). Elemental analysis calcd (%, for $C_{42}H_{71}Ag_2N_{14}O_{10}$) C 43.95, H 6.23, N 17.08; found C 43.58, H 6.32, N 17.42. Selected IR peaks ($cm^{-1}$): 3444(w), 3201(s), 3077(m), 2940(s), 1725(m), 1561(s), 1410(s), 1255(w), 1168(m), 1015(s), 783(w).

*$[Ag_2(bpz)_4(sub)\cdot 7H_2O]_n$ (**6**).* Synthesis of complex **6** was similar to that of **2** but using $H_2$sub (34.8 mg, 0.2 mmol) instead of $H_2$suc (23.6 mg, 0.2 mmol). The pH values of system are 4.40 and 4.27 before and after the solvothermal reaction. Colorless needlelike crystals of **6** were isolated by filtration, washed with $H_2O$, and dried in air (yield 61% based on bpz). Elemental analysis calcd (%, for $C_{48}H_{82}Ag_2N_{16}O_{11}$) C


dx.doi.org/10.1021/cg401805x | Cryst. Growth Des. XXXX, XXX, XXX–XXX

**Table 1. Crystal Data and Structure Refinement Parameters of Complexes 1−7**

| compound | **1*L*** | **1*R*** | **2** | **3** | **4** | **5** | **6** | **7** |
|---|---|---|---|---|---|---|---|---|
| formula | $C_{43}H_{58}Ag_2N_{16}O_4$ | $C_{43}H_{58}Ag_2N_{16}O_4$ | $C_{17}H_{23}AgN_6O_2$ | $C_{30}H_{41}Ag_2N_{10}O_4$ | $C_{31}H_{43}Ag_2N_{10}O_4$ | $C_{42}H_{71}Ag_2N_{14}O_{10}$ | $C_{48}H_{68}Ag_2N_{16}O_4$ | $C_{39}H_{63}Ag_2N_{12}O_{7.5}$ |
| $F_w$ | 1078.79 | 1078.79 | 451.28 | 821.47 | 835.49 | 1147.87 | 1148.92 | 1035.75 |
| $T$, K | 298(2) | 298(2) | 298(2) | 298(2) | 298(2) | 120(2) | 298(2) | 298(2) |
| cryst syst | tetragonal | tetragonal | tetragonal | orthorhombic | orthorhombic | monoclinic | monoclinic | monoclinic |
| space group | $P4_12_12$ | $P4_32_12$ | $I4_1/acd$ | $Aba2$ | $Aba2$ | $C2/c$ | $C2/c$ | $C2/c$ |
| $a$, Å | 23.139(2) | 22.943(3) | 23.1175(6) | 23.3260(6) | 22.712(5) | 30.817(6) | 49.040(10) | 35.034(14) |
| $b$, Å | 23.139(2) | 22.943(3) | 23.1175(6) | 32.240(2) | 34.599(8) | 10.354(2) | 10.368(2) | 10.387(4) |
| $c$, Å | 10.5768(19) | 10.4944(13) | 28.1024(15) | 9.8621(14) | 9.858(2) | 34.565(7) | 34.821(12) | 30.465(13) |
| $\beta$, deg | 90.00 | 90.00 | 90.00 | 90.00 | 90.00 | 98.748(4) | 134.615(3) | 113.813(7) |
| $V$, Å$^3$ | 5663.1(13) | 5524.2(9) | 15018.5(10) | 7416.6(12) | 7747(3) | 10901(4) | 12603(6) | 10142(7) |
| $Z$ | 4 | 4 | 32 | 8 | 8 | 8 | 8 | 8 |
| $\rho_{calc}$, mg/mm$^3$ | 1.265 | 1.297 | 1.597 | 1.471 | 1.433 | 1.399 | 1.211 | 1.357 |
| $\mu$, mm$^{-1}$ | 0.741 | 0.760 | 1.098 | 1.102 | 1.056 | 0.781 | 0.670 | 0.827 |
| $F(000)$ | 2216.0 | 2216.0 | 7360.0 | 3336.0 | 3400.0 | 4760.0 | 4752.0 | 4280.0 |
| reflns measd | 27 600 | 21 914 | 35 646 | 22 656 | 18 406 | 26 298 | 30 294 | 24 317 |
| unique reflns | 4983 | 4836 | 3320 | 6391 | 6738 | 9581 | 11 036 | 8929 |
| $R_{int}$ | 0.0900 | 0.0978 | 0.0463 | 0.0306 | 0.0986 | 0.0994 | 0.1380 | 0.0687 |
| params | 301 | 302 | 266 | 424 | 432 | 614 | 649 | 557 |
| GOF on $F^2$ | 1.028 | 1.254 | 1.021 | 1.055 | 0.969 | 0.966 | 0.878 | 1.006 |
| $R_1$ $[I > 2\sigma(I)]^a$ | 0.0785 | 0.0878 | 0.0307 | 0.0474 | 0.0540 | 0.0534 | 0.0743 | 0.0563 |
| $wR_2$ $[I > 2\sigma(I)]^b$ | 0.1793 | 0.2155 | 0.0737 | 0.1154 | 0.0945 | 0.0996 | 0.1844 | 0.1321 |
| $R_1$ [all data]$^a$ | 0.1005 | 0.1209 | 0.0433 | 0.0605 | 0.1278 | 0.1098 | 0.1234 | 0.1222 |
| $wR_2$ [all data]$^b$ | 0.1906 | 0.2276 | 0.0816 | 0.1260 | 0.1204 | 0.1232 | 0.2001 | 0.1636 |

$^a R_1 = \sum||F_o| - |F_c||/\sum|F_o|$. $^b wR_2 = [\sum w(F_o^2 - F_c^2)^2]/\sum w(F_o^2)^2]^{1/2}$.



dx.doi.org/10.1021/cg401805x | Cryst. Growth Des. XXXX, XXX, XXX−XXX

45.22, H 6.48, N 17.56; found C 42.08, H 6.32, N 17.01. Selected IR peaks ($cm^{-1}$): 3201(m), 2929(m), 1567(s), 1410(s), 1287(w), 1256(w), 1168(w), 1014(w), 782(w), 697(w), 404(w).

*$[Ag_2(bpz)_3(aze)\cdot 3.5H_2O]_n$ (**7**).* A mixture of $Ag_2O$ (23.2 mg, 0.1 mmol), bpz (19 mg, 0.1 mmol), $H_2$aze (18.8 mg, 0.1 mmol), and 6 mL of $H_2O$ was heated to 180 °C in 10 h in a 25 mL Teflon-lined reaction vessel, kept 180 °C for 50 h, and then slowly cooled to 30 °C in 13 h. The pH values of system are 4.07 and 4.14 before and after the solvothermal reaction. Colorless needlelike crystals of **7** were isolated by filtration, washed with $H_2O$, and dried in air (yield 35% based on bpz). Elemental analysis calcd (%, for $C_{39}H_{63}Ag_2N_{12}O_{7.5}$) C 45.23, H 6.13, N 16.23; found C 45.09, H 6.32, N 16.91. Selected IR peaks ($cm^{-1}$): 3201(m), 2928(m), 1565(s), 1408(s), 1307(w), 1169(w), 1015(w), 780(w).

**X-ray Crystallography.** Single crystals of the complexes **1**−**7** with appropriate dimensions were chosen under an optical microscope and quickly coated with high vacuum grease (Dow Corning Corporation) before being mounted on a glass fiber for data collection. Data for them were collected on a Bruker Apex II CCD diffractometer with graphite-monochromated Mo K$\alpha$ radiation source ($\lambda$ = 0.71073 Å). A preliminary orientation matrix and unit cell parameters were determined from 3 runs of 12 frames each; each frame corresponds to a 0.5° scan in 8 s, followed by spot integration and least-squares refinement. For **1**−**7**, data were measured using $\omega$ scans of 0.5° per frame for 12 s until a complete hemisphere had been collected. Cell parameters were retrieved using SMART software and refined with SAINT on all observed reflections.[13] Data reduction was performed with the SAINT software and corrected for Lorentz and polarization effects. Absorption corrections were applied with the program SADABS.[14] In all cases, the highest possible space group was chosen. All structures were solved by direct methods using SHELXS-97 and refined on $F^2$ by full-matrix least-squares procedures with SHELXL-97.[15] Atoms were located from iterative examination of difference $F$-maps following least-squares refinements of the earlier models. Hydrogen atoms were placed in calculated positions and included as riding atoms with isotropic displacement parameters 1.2−1.5 times $U_{eq}$ of the attached C atoms. Pertinent crystallographic data collection and refinement parameters are collated in Table 1. Selected bond lengths and angles are collated in Table S1, Supporting Information. Hydrogen bond parameters are collated in Table S2, Supporting Information. Topological analysis of coordination networks in all complexes was performed with the program package TOPOS.[16]

## RESULTS AND DISCUSSION

**Synthesis and General Characterization.** The synthesis of **1**−**7** was performed in 25 mL Teflon-lined stainless steel autoclave under solvothermal conditions. In the synthesis, the isolations and yields were heavily influenced by the kinds of silver salt, temperature, reactant molar ratio, and auxiliary solvent (Table S4, Supporting Information). We first attempted to synthesize all complexes in the same reaction conditions (solvent, water; reactant molar ratio of $Ag_2O$/bpz/dicarboxylate, 1:2:2; temperature, 180 °C), which could only yield good single crystals of complexes **2**, **3**, **4**, and **6**. Complex **1** was exclusively obtained in the presence of additional pyridine (3 drops). The reaction temperature of 180 °C seems to be the best temperature for the preparation of **2**, **3**, **4**, **6**, and **7**. However, for **1** and **5**, the dicarboxylates were *in situ* decomposed to $OAc^-$ anion resulting in a known complex, $[Ag(bpz)_2(OAc)\cdot 5.4H_2O]_n$,[11e] at 180 °C. The high temperature may be responsible for the undesired decomposition of $H_2$mal and $H_2$pim, so we lowered temperature and successfully synthesized **1** and **5** at 120 °C. Reactant ratios of $Ag_2O$/bpz/dicarboxylate of 1:2:2 are suitable for synthesis of **1**−**6**, but complex **7** was exclusively obtained in the ratio of 1:1:1. When $AgNO_3$ or $AgClO_4$ were used in this system, a known complex, $[Ag_4(bpz)_5(NO_3)_4]_n$ or $[Ag(bpz)(ClO_4)]_n$, could be isolated.[11b] So $Ag_2O$ was used instead of $AgNO_3$ or other common Ag(I) salts in order to promote coordination of the dicarboxylates instead of small anions to the Ag(I) centers. Powder X-ray diffraction (PXRD) has been used to check the phase purity of the bulk samples in the solid state. For complexes **1**−**7**, the measured PXRD patterns closely match the simulated patterns generated from the results of single-crystal diffraction data (Figure S1, Supporting Information), indicative of pure products.

**Structure Descriptions.** *$[Ag_2(bpz)_4(mal)\cdot 7H_2O]_n$ (**1*L* and *1*R*).* The structures of **1** were characterized by single crystal X-ray diffraction analyses, and the results showed that **1** contains single crystals of **1*L*** and **1*R*** with the chiral tetragonal space group $P4_12_12$ (Flack parameter 0.07(8)) and $P4_32_12$ (Flack parameter 0.06(8)), respectively, indicating a homochiral crystal with all helices of the same left- or right-handness. In order to ascertain the spontaneous resolution of **1**, six crystals randomly picked from a single batch were refined using single crystal X-ray diffraction data. The space group of three crystals is $P4_12_12$, whereas that of the other three is $P4_32_12$, and the Flack prarmeters of them are close to zero (Table S4, Supporting Information). The enantiomeric nature of **1*L*** and **1*R*** can be simply represented by their mirror structures (Figure 1). Since **1*L*** and **1*R*** are enantiomers, the structure of **1*L*** is detailed here.

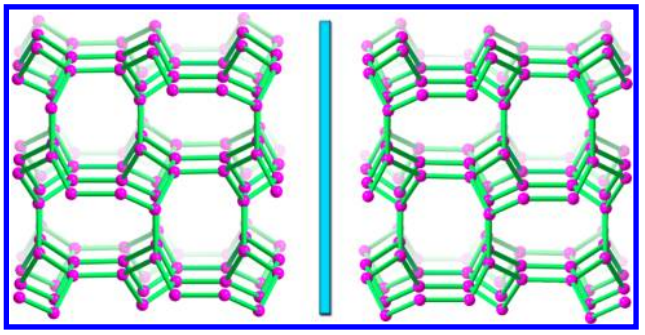

**Figure 1.** Schematic representations of mirror images of 3D chiral $SrSi_2$ net of **1*L*** and **1*R***.

The asymmetric unit of **1*L*** contains one crystallographically independent Ag(I) ion, two bpz ligands, and one-half of a mal anion, as well as four disordered lattice water molecules. The C22 atom was passed by the crystallographically *C*2 axis. As shown in Figure 2a, the Ag1 is coordinated by three N atoms from three bpz ligands and one O atom from mal, giving a $AgN_3O$ distorted tetrahedral coordination geometry. The Ag−N and Ag−O bond lengths are in the normal ranges.[17,18] The distortion of the tetrahedron can be indicated by the calculated value of the $\tau_4$ parameter introduced by Houser[19] to describe the geometry of a four-coordinate metal system, which is 0.76 for Ag1 (for ideal tetrahedron $\tau_4$ = 1). The interpyrazole dihedral angles for two different bpz ligands are 62.8(8)° and 65.6(7)°, respectively. Two distinct bpz ligands display *exo*-bidentate and *exo*-monodentate coordination modes, respectively. The mal anion is in a $(\kappa^1\text{-}\kappa^0)\text{-}(\kappa^1\text{-}\kappa^0)\text{-}\mu_2$ coordination mode. The uncoordinated O atoms are hydrogen-bonded to the N atoms of bpz. The bidentate bridging bpz and mal link the Ag(I) ions into a 3D network. It is fascinating that there are two kinds of helical chains, one with a left-handed $4_1$ screw axis and another with a right-handed $2_1$ screw axis in **1*L***, and it is the opposite phenomenon in **1*R***. Evidently, the original


dx.doi.org/10.1021/cg401805x | Cryst. Growth Des. XXXX, XXX, XXX−XXX

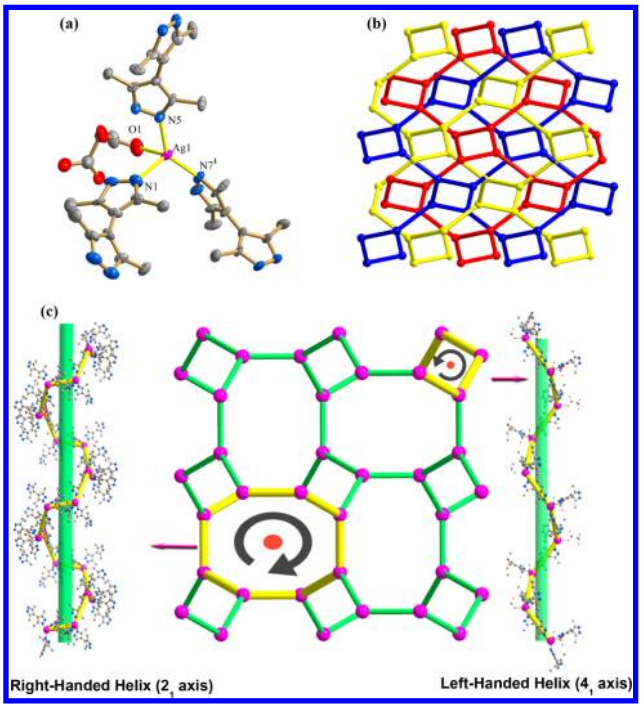


**Figure 2.** (a) The coordination environment of Ag(I) ion in **1*L*** with the thermal ellipsoids at 30% probability level. Symmetry code: (i) $-y + 3/2, x - 1/2, z - 3/4$. (b) Ball-and-stick representation of the 3D 3-fold interpenetrated **srs** net viewed along the *a* axis (networks individually colored). (c) Ball-and-stick representations of the helical chains in the single 3D net viewed along the *c* axis (a right-handed helix in **1*L*** with a $2_1$ helical axis and a left-handed helix in **1*L*** with a $4_1$ helical axis).

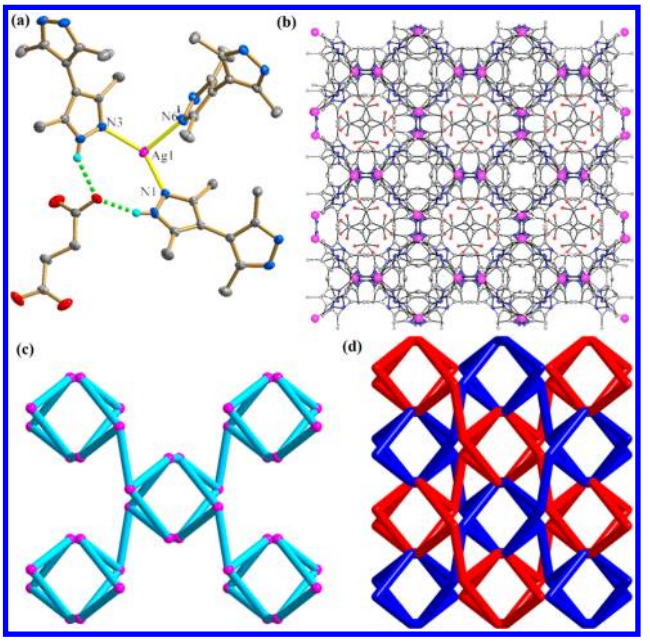


**Figure 3.** (a) The coordination environment of Ag(I) ion in **2** with the thermal ellipsoids at 30% probability level. Symmetry code (i) $y - 1/4, -x + 5/4, -z + 3/4$. (b) Ball-and-stick representation of the 3D framework (purple ball, Ag; blue ball, N; red ball, O; gray ball, C). (c) Ball-and-stick view of simplified single **dia-f** net. (d) Schematic view of the simplified 2-fold interpenetrated network (networks individually colored).

chirality of the complex is due to the screw coordination arrangement of the achiral ligand around the Ag(I) centers (Figure 2c).

Topologically, each Ag(I) atom has been linked by four ligands; however, due to existence of one monodentate bpz, each Ag(I) atom can be simplified into a 3-connected node. The whole network can thus be represented topologically by 3-connected (10,3)-a net. It has an extended Schläfli symbol of $\{10^5\cdot10^5\cdot10^5\}$, which is assigned to a $SrSi_2$ (**srs**) topology (Figure 2b).[20] This net is one of the five regular 3-periodic nets and is the solely chiral one. Three equivalent nets adopt 3-fold interpenetration to minimize the large voids in the single net. According to Blatov's classification,[21] the interpenetration can be classified as type class Ia, $Z_t = 3$, which means three identical interpenetrated nets are generated by only translations with the translating vectors of [0, 0, 1]. Despite interpenetration, **1** still possesses free void space estimated to be about 864.4 Å$^3$, that is, 15.3% of the unit cell.

*$[Ag_2(bpz)_3(suc)]_n$ (**2**).* When suc was used, we obtained **2** as a 3D 2-fold interpenetrated **dia-f** networks. Complex **2** crystallized in a tetragonal crystal system with space group of $I4_1/acd$, and there is one crystallographically independent Ag(I) ion, one and a half of bpz ligands, and a half of uncoordinated suc anion. As shown in Figure 3a, the Ag1 is located in the triangular coordination geometry with an $AgN_3$ environment. One of bpz ligand was passed by a *C*2 axis through the midpoint of C3−C3$^{iv}$ bond (symmetry code (iv) $-x + 1/2, y, -z + 1$). The interpyrazole dihedral angles for two different bpz ligands are 82.18(19)° and 73.64(2)°, respectively. The shortest Ag(I)···Ag(I) separation is 3.0246(5) Å, which is shorter than the sum of Ag(I) van der Waals radii (3.44 Å), indicating the presence of ligand-unsupported argentophilicity.[22] The bpz ligands with an *exo*-bidentate mode extend the Ag(I) centers into a 3D 2-fold interpenetrated network, whereas the suc did not participate in the construction of the resultant network and only as counteranion located in the void of the 3D network through the N−H···O hydrogen bonds.

Better insight into the complicated 3D architecture can be achieved by topology analysis. The bpz bridging ligands are omitted due to the linear geometry, whereas the Ag atoms are linked by three bpz ligands, so the single 3D network could be simplified to a rare $\{4\cdot14^2\}$ net, which is assigned to the **dia-f** net, as displayed in Figure 3b. An interesting feature of this net is the existence of the isolated hexagonal single helices running along the *a* axis, each of which further connects to four neighboring helices by sharing a common edge (Figure 3c). Two equal nets are 2-fold interpenetrating (Figure 3d) and interlocked with each other through Ag(I)···Ag(I) interactions. In **2**, the interpenetration can be classified as type class IIa, which means that two identical interpenetrated nets are generated by means of space group interpenetration symmetry element, here an inversion center, and no interpenetrating translations are allowed in this kind of interpenetration. The present net is strongly distorted and differs from the regular **dia-f** net, whose symmetrical configuration is normally $I4_1/amd$ of the tetragonal cell.[23] Alternatively, if the Ag(I)···Ag(I) interaction is included in the simplification of the net, each Ag(I) become to a 4-connected node; thus a noninterpenetrated 4-connected **upd** net with Schläfli symbol of $\{4\cdot6^3\cdot8^2\}$ is produced (Figure S2, Supporting Information).

*$[Ag_4(bpz)_5(glu)_2]_n$ (**3**) and $[Ag_4(bpz)_5(adip)_2]_n$ (**4**).* Both complexes **3** and **4** are similar 2D + 2D → 2D $6^3$-**hcb** layer featuring 3-fold parallel interpenetration mode. Herein, we only


dx.doi.org/10.1021/cg401805x | *Cryst. Growth Des.* XXXX, XXX, XXX−XXX

discussed the structure of **3** in detail. Complex **3** crystallizes in the orthorhombic space group *Aba*2, and the asymmetric unit consists of two crystallographically independent Ag(I) ions, two and a half bpz, and one glu anion. Both Ag(I) ions locate in triangular coordination geometry with similar coordination environment of $AgN_3$ (Figure 4a). The interpyrazole dihedral

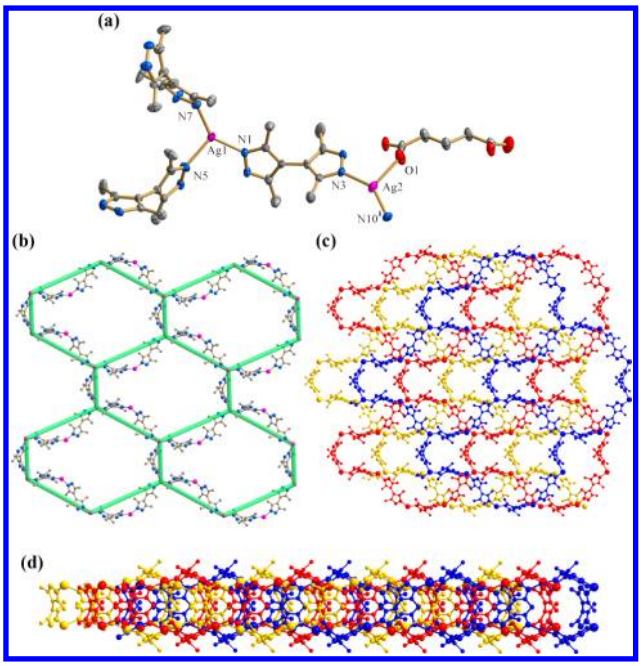


**Figure 4.** (a) The coordination environments of Ag(I) ions in **3** with the thermal ellipsoids at 30% probability level. Symmetry code (i) $-x + 1, -y + 1/2, z + 3/2$. (b) Presentation of 2D $6^3$-**hcb** network (purple ball, Ag; red ball, O; blue ball, N; gray ball, C). (c, d) The 3-fold 2D + 2D → 2D parallel interpenetrated $6^3$-**hcb** networks viewed along two different directions (networks individually colored).

angles for three bpz ligands are 72.4(4)°, 64.4(5)°, and 73.5(4)°, respectively. All bpz ligands adopt *exo*-bidentate coordination modes to extend the Ag(I) ions, generating a 2D layer. The glu anion just monodentately coordinates to the Ag(I) ion; thus it does not contribute to the extension of the 2D layer to higher dimensionality.

The single 2D layer could be simplified to a wavy $6^3$-**hcb** network (Figure 4b). The large metal−organic hexagons are sustained by two shorter Ag−bpz−Ag linkers (Ag···Ag = 9.941(1) Å) and four longer Ag−bpz−Ag−bpz−Ag linkers (Ag···Ag = 17.467(2) Å). Due to the large windows in this layer, three identical layers are penetrated with each other with a 2D + 2D → 2D parallel interpenetrated mode (Figure 4c).[24]

*$[Ag_4(bpz)_7(pim)_2 \cdot 12H_2O]_n$* ***(5)***. Complex **5** crystallizes in the monoclinic space group *C*2/*c*, and the asymmetric unit consists of two crystallographically independent Ag(I) ions, three and a half bpz, one pim anion, and six lattice water molecules. Both Ag(I) ions locate in distorted $AgN_3O$ tetrahedral coordination geometry with $\tau_4$ parameters of 0.76 and 0.77 for Ag1 and Ag2, respectively (Figure 5a). One of the bpz ligands is passed by a *C*2 axis through the midpoint of C33−C33$^{viii}$ bond (symmetry code (viii) $-x + 1, y, -z + 3/2$). The interpyrazole dihedral angles for four bpz ligands are 58.7(3)°, 70.9(3)°, 65.3(3)°, and 69.3(3)°, respectively. Among four distinct bpz ligands, three display an *exo*-bidentate binding mode and the remaining has an *exo*-monodentate coordination mode. The pim anion bidentately coordinates to the Ag(I) ion, which combines

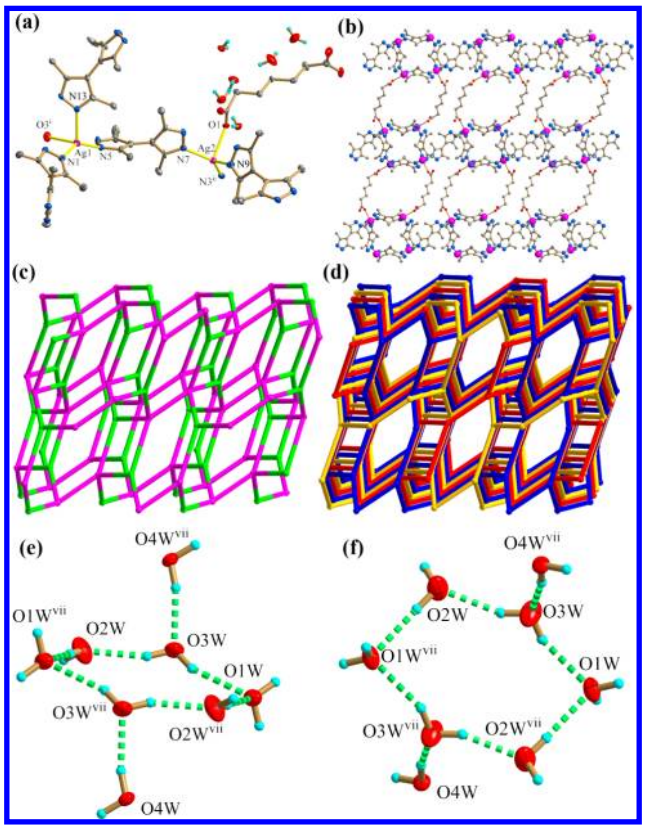


**Figure 5.** (a) The coordination environments of Ag(I) ions in **5** with the thermal ellipsoids at 30% probability level. (b) Presentation of 3D network (purple ball, Ag; red ball, O; blue ball, N; gray ball, C). (c) Simplified 3D (3,4)-connected **3,4T1** topology (green ball, 3-connected node; purple ball, 4-connected node). (d) Simplified 3D 3-fold interpenetrated (3,4)-connected **3,4T1** network (networks individually colored). (e, f) octamer water cluster viewed along two different directions. Symmetry codes: (i) $x, -y + 1, z + 1/2$; (ii) $-x + 1/2, y + 3/2, -z + 3/2$; (vii) $-x + 1, -y + 1, -z + 1$).

with the *exo*-bidentate bpz ligand to extend the Ag(I) ions into the resulting 3D network (Figure 5b).

Although both Ag1 and Ag2 are four-coordinated by one O and three N atoms, Ag2 belongs to a 3-connected node due to the existence of the monodentate bpz ligand. In fact, this 3D net contains 3- and 4-connected metal centers, whereas both bpz and pim are linear spacers, so this 3D network could be simplified a (3,4)-connected **3,4T1** topology with Schläfli symbol of $\{4\cdot6\cdot8\}\{4\cdot6^2\cdot8^3\}$ (Figure 5c). Three equivalent nets adopt 3-fold interpenetration to minimize the large voids in the single net (Figure 5d). The interpenetration can be classified as type class Ia, $Z_t = 3$, which means three identical interpenetrated nets are generated by the translating vectors of [0, 1, 0].

Despite interpenetration, complex **5** still possesses large void space, which is filled by the well-resolved octanuclear water. As shown in Figure 5e,f, the centrosymmetric octamer water cluster consists of four water molecules (O1W−O4W) and their centrosymmetric equivalents. The short contacts and the reasonable angles between them indicate the existence of hydrogen bonds, which drive the formation of a hydrophilic octamer water cluster. The water octamer consists of a chairlike hexamer in the core and two extra water molecules dangling at two diagonal vertices of the chair with a distance of 8.434(5) Å, which is structurally analogous to the simple hydrocarbon


dx.doi.org/10.1021/cg401805x | *Cryst. Growth Des.* XXXX, XXX, XXX−XXX

(1*r*,4*r*)-1,4-dimethylcyclohexane. In the cyclic hexamer, O1W just acts as double hydrogen bond acceptor, O2W acts as single hydrogen bond acceptor and donor, and O3W acts as double hydrogen bond donor; as a result, the hydrogen bonding motif is $R_6^4(12)$, according to the graphset analysis nomenclature.[25] The O1W deviates from the plane determined by O2W, O3W, O2W$^{vii}$, and O3W$^{vii}$ by 0.68 Å. As listed in Table S3, Supporting Information, the O···O distances in the octamer water cluster fall in the range of 2.676(6)−2.872(7) Å with an average value of 2.761(6) Å, compared with 2.76 Å (−90 °C) in hexagonal ($I_h$) ice[26] or 2.74 Å in cubic ($I_c$) ice.[27] This octamer water cluster was stabilized in the 3D network through $O_{water}$−H···$O_{carboxyl}$ hydrogen bonds.

*$[Ag_2(bpz)_4(sub)\cdot 7H_2O]_n$ (**6**) and $[Ag_2(bpz)_3(aze)\cdot 3.5H_2O]_n$ (**7**).* When longer $H_2$sub and $H_2$aze ligands were used, we obtained **6** and **7** as similar 2D + 2D → 2D **fes** layers featuring 3-fold parallel interpenetration mode, although they have different metal/ligand ratios. In the asymmetric unit of **6**, there are two crystallographically unique Ag(I) atoms, four bpz, one sub, and seven lattice water molecules. Both Ag(I) atoms are in tetrahedral $AgN_3O$ coordination geometry with almost equal $\tau_4$ parameters of 0.76 (Figure S3, Supporting Information). Two of four unique bpz ligands are *exo*-bidentate and the remaining two are monodentate. The bidentate sub anion combines with the *exo*-bidentate bpz to extend the Ag(I) ion to a 2D layer. The asymmetric unit of **7** contains two crystallographically unique Ag(I) atoms, three bpz, one aze, and three and a half lattice water molecules. As shown in Figure 6a, Ag1 is in a distorted $AgN_3O$ tetrahedral coordination geometry with $\tau_4$ parameter of 0.76, whereas Ag2 locates in a $AgN_2O$ triangular geometry. Two of three bpz are *exo*-bidentate, and the third one is monodentate. The dihedral angles formed between two pyrazole rings of the bpz ligand are 72.0(4)°, 62.0(4)°, and 66.6(4)°, respectively. The aze anion bidentately coordinates to Ag(I) ion and combines with the *exo*-bidentate bpz to extend the Ag(I) ion to a 2D layer. The single 2D layer in both **6** and **7** could be simplified to a **fes** network with Schläfli symbol of $\{4\cdot 8^2\}$ (Figure 6b), which is composed of a 3-connected Ag(I) node and metal−organic tetragons and octagons sustained by shorter Ag−bpz−Ag linkers and four larger Ag−aze−Ag linkers. Due to the large octagonal windows in this layer, three identical layers are penetrated with each other with a 2D + 2D → 2D parallel interpenetrated mode (Figure 6c).

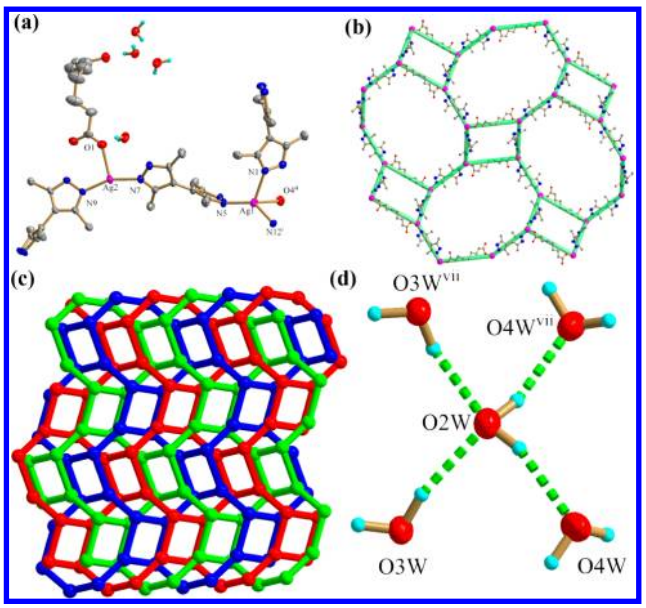


**Figure 6.** (a) The coordination environments of Ag(I) ions in **7** with the thermal ellipsoids at 30% probability level. (b) Presentation of 2D **fes** network (purple ball, Ag; red ball, O; blue ball, N; gray ball, C). (c) The 3-fold 2D + 2D → 2D parallel interpenetrated **fes** network (networks individually colored). (d) The water pentamer. Symmetry codes: (i) $-x + 1/2, y - 3/2, -z + 1/2$, (ii) $-x + 1, -y + 1, -z + 1$, (vii) $-x + 1, y, -z + 3/2$).

Another striking feature of **7** is the existence of a discrete pentamer water cluster, which is different from the theoretically predicted most stable structures for the possible water pentamers with several configurations including "ring", "envelope", and "cage". This pentamer water cluster possesses a $C_2$ symmetry and is an acyclic structure composed of central O2W, two water molecules (O3W and O4W), and their centrosymmetric equivalents. The O2W locates in a tetrahedral geometry and acts as double hydrogen bond acceptor and donor to bind with four other water molecules, giving a seesaw-like configuration. The O···O distances in the pentamer water cluster are 2.776(5) and 2.795(6) Å, respectively. Although some water pentamers as subunits are found in infinite water aggregates such as 1D T5(2) water tape, experimentally identified discrete pentamer water clusters are very rare.

**Effects of Length of Dicarboxylate on the Structures.** In this study, seven aliphatic dicarboxylate ancillary ligands differing in methylene chain lengths between two terminal carboxyl groups have been used to investigate the formation of products in the Ag(I)/bpz system under similar reaction conditions. The bpz ligand has similar length and *exo*-bidentate or *exo*-monodentate coordination mode in these networks (Table S5, Supporting Information), which indicates that the bpz ligands have negligible effect on the final networks. As expected, the different lengths of the flexible aliphatic dicarboxylates have an important influence on the final networks (Scheme 2). In **1**, the mal ligand possesses a shorter $-(CH_2)_n-$ length ($n$ = 1) and less flexibility, which makes it easy to connect the Ag(I) ions forming a 3D chiral 3-fold interpenetrated network with **srs** topology. With increase of the $-(CH_2)_n-$ length ($n$ = 2), the 2-fold interpenetrated network with **dia-f** topology in **2** is obtained, though suc does not coordinated to any metal centers. Upon further elongation of the $-(CH_2)_n-$ length ($n$ = 3 and 4), 2D + 2D → 2D parallel interpenetrated $6^3$-**hcb** networks are observed in **3** and **4**. Although both glu and adip monodentately coordinate to the Ag(I) ion and they contribute nothing to the extension of the 2D layer to higher dimensionality, their dimensions and conformations undoubtedly drive them to the different structures from **1** and **2**. When pim ($n$ = 5 in $-(CH_2)_n-$ chain) was used in this system, a novel (3,4)-connected binodal 3-fold interpenetrated **3,4T1** topology is obtained for **5**. When longer sub and aze were used, we obtained another relatively less encountered 3-connected 2D layer showing 2D + 2D → 2D 3-fold parallel interpenetrated **fes** layer for **6** and **7**.

**Thermal Analysis.** The TG analysis was performed in $N_2$ atmosphere (100 mL min$^{-1}$) on polycrystalline samples of CPs **1**−**7**. The temperature was ramped at a rate of 10 °C min$^{-1}$ from 25 to 800 °C. The TG curves are shown in Figure 7. For **1**, the first weight loss of 9.8% (calcd 10.5%) at 30−183 °C corresponds to loss of lattice water molecules; then organic ligands were gradually decomposed above 183 °C. Complexes **2**−**4** are thermally stable up to around 235 °C, and mass losses occur above 250 °C due to the decomposition of organic


dx.doi.org/10.1021/cg401805x | *Cryst. Growth Des.* XXXX, XXX, XXX−XXX

**Scheme 2. Structural Variation as a Function of Dicarboxylates for 1−7**

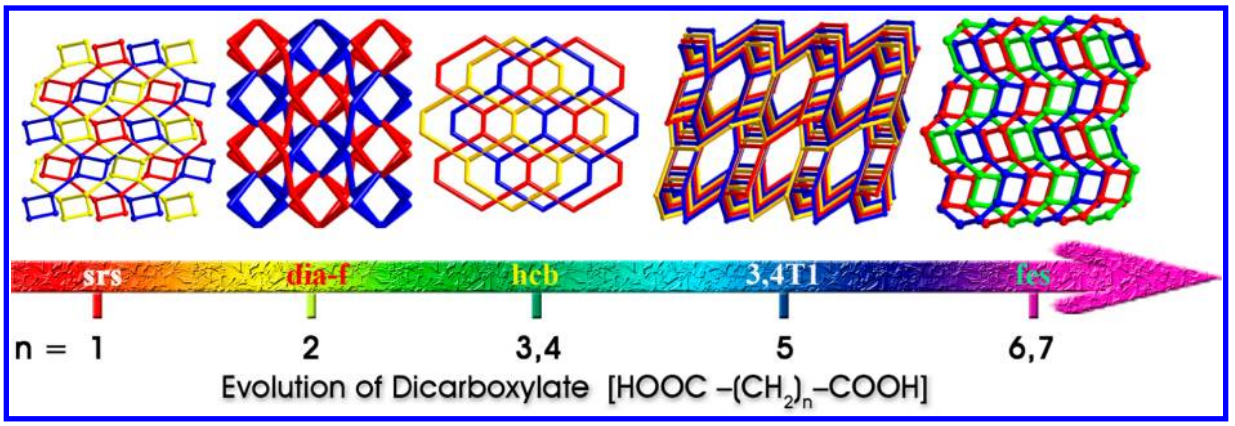


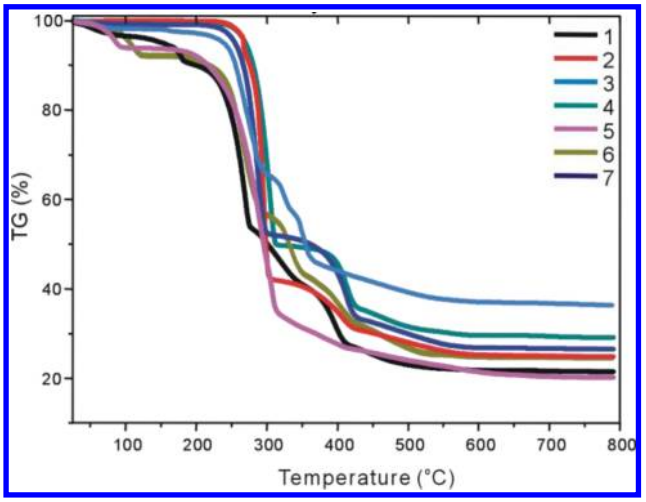


**Figure 7.** TGA curves for CPs **1**−**7**.

ligands. Complex **5** completely loses its lattice water molecules at 91 °C (found 9.7%; calcd 9.4%); then the dehydrated framework stabilizes to 173 °C before the decomposition of organic ligands occurs. Complex **6** completely loses its lattice water molecules at 120 °C (found 9.2%; calcd 9.9%); then the dehydrated framework stabilizes to 195 °C before the decomposition occurs. For **7**, the first weight loss of 5.5% in the range of 30−150 °C corresponds to the loss of water molecules; then the host framework begins to collapse, with accompanying loss of the organic ligand.

The existence of wide plateau areas in the TGA plots of **5** (95−170 °C) and **7** (90−190 °C) indicates that they would be amenable to a dehydration−rehydration study. The variable temperature PXRD of **5** and **7** and room temperature PXRD patterns for rehydrated samples are shown in Figure S4, Supporting Information. For **5** and **7**, they have similar thermal stability upon heating, and the dehydration−rehydration behaviors of them are irreversible. For **5**, PXRD pattern at 60 °C still could be matched with the simulated pattern, indicating that the framework could be retained, though the dehydration has occurred at that temperature. Upon further heating to 90 °C, the slight shift of diffraction peaks to high degree was observed, but most of the peaks still exist, indicating that some distortion of network happened. At 150 °C, the PXRD patterns completely changed to unknown phase indicating the collapse of the framework upon exclusion of the water cluster but without loss of any compositions of host framework. The dehydrated sample could not revert back to the original solid by rehydration in humid atmosphere at room temperature for 12 h, as indicated by the PXRD results. These observations clearly indicate that water clusters are difficult to rearrange in the crystal lattice of the dehydrated sample.

**UV−Vis Spectra and Photoluminescence Properties.** The absorption spectra of free bpz and **1**−**7** were measured in solid state at room temperature. As shown in Figure S6, Supporting Information, all complexes show the high-energy absorption bands at ca. 240−350 nm, which are ascribed to the intraligand $\pi \rightarrow \pi^*$ transitions of the bpz moiety. The photoluminescence properties of complexes **1**−**7** were investigated in the solid state at room temperature and 77 K, respectively. Upon excitation ($\lambda_{ex}$ = 365 nm) at room temperature, solid samples of **1**, **3**, **4**, **6**, and **7** exhibit similar luminescence in the blue−green region with centers at ca. 465 nm, whereas emission of **5** is centered at 454 nm (Figure 8).

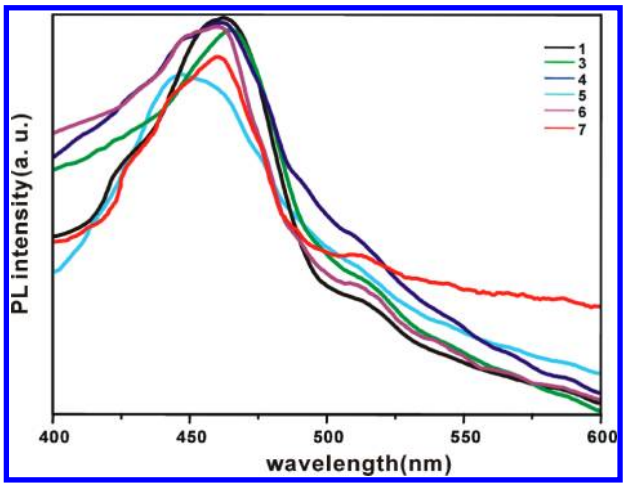


**Figure 8.** The photoluminescence of **1** and **3**−**7** under 365 nm excitation at 298 K.

Complex **2** shows no detectable emission at room temperature, which may be due to the loss of energy by nonradiative decay caused by disordered uncoordinated suc anion. These emission bands resemble the emission peak of free bpz ($\lambda_{max}$ = 342 nm)[28] and thus can be preferably ascribed to ligand-centered transitions.[29] A slightly different emission peak arises from the different coordination environments of Ag(I) centers. When the complexes are cooled to 77 K, the emission intensities of **1** and **3**−**7** are enhanced to different degrees, but no obvious


dx.doi.org/10.1021/cg401805x | Cryst. Growth Des. XXXX, XXX, XXX−XXX

emission shifts are observed. The enhanced emission at low temperature may be caused by the enhanced rigidity and faster intersystem crossing process by the presence of the heavy-metal ion upon cooling, which effectively reduces the loss of energy by nonradiative decay.[30]

## CONCLUSIONS

In conclusion, we have constructed seven novel silver(I) coordination networks with mixed flexible 3,3′,5,5′-tetramethyl-4,4′-bipyrazole and different aliphatic dicarboxylates. As the length of alkyl chain of dicarboxylates increases from one to seven, five different structural motifs, including 3-fold interpenetrated chiral $SrSi_2$, 2-fold interpenetrated **dia-f**, 3-fold parallel interpenetrated 2D + 2D → 2D $6^3$-**hcb**, 3-fold interpenetrated **3,4T1**, and 3-fold parallel interpenetrated 2D + 2D → 2D **fes** nets, are obtained. A pair of enantiomorphs (**1*L*** and **1*R***) was recognized by spontaneous resolution upon crystallization without any chiral source, which provides new opportunities for chiral materials. Interestingly, a well-resolved octanuclear water and a rare seesaw-like pentanuclear water cluster are captured in the voids of **5** and **7**, respectively. This work systematically disclosed and demonstrated how the structure changed with the elongation of alkyl chain of dicarboxylates. Furthermore, the solid-state photoluminescence properties of the **1**−**7** were investigated at 298 and 77 K.

## ASSOCIATED CONTENT

### Supporting Information

Crystallographic data in CIF format, powder X-ray diffraction (PXRD) patterns for **1**−**7**, selected bond lengths and angles and hydrogen bond parameters for **1**−**7**, crytallographic data for the randomly selected crystals of **1**, summary of synthesis conditions for **1**−**7**, and IR and UV−vis spectra of **1**−**7**. This material is available free of charge via the Internet at http://pubs.acs.org. CIF files have also been deposited at the Cambridge Crystallographic Data Centre and may be obtained from http://www.ccdc.cam.ac.uk by citing deposition numbers 977473−977479 for **1**−**7**.

## AUTHOR INFORMATION

### Corresponding Authors

*E-mail: dfsun@upc.edu.cn (D.F.S.).
*E-mail: dsun@sdu.edu.cn (D.S).

### Notes

The authors declare no competing financial interest.

## ACKNOWLEDGMENTS

This work was supported by the NSFC (Grant Nos. 21201110 and 21271117), the Special Funding of China Postdoctoral Science Foundation (Grant 2013T60663), and Research Award Fund for Outstanding Middle-aged and Young Scientist of Shandong Province (Grant BS2013CL010). X. P. Wang acknowledges the Youth Award of Shandong Province (Grant No. 2007BS03033) for financial assistance.

## REFERENCES

(1) (a) Zhang, Z. J.; Wojtas, L.; Eddaoudi, M.; Zaworotko, M. J. *J. Am. Chem. Soc.* **2013**, *135*, 5982. (b) Rusanov, E. B.; Ponomarova, V. V.; Komarchuk, V. V.; Stoeckli-Evans, H.; Fernandez-Ibanez, E.; Stoeckli, F.; Sieler, J.; Domasevitch, K. V. *Angew. Chem., Int. Ed.* **2003**, *42*, 2499. (c) Yin, Z.; Wang, Q. X.; Zeng, M. H. *J. Am. Chem. Soc.* **2012**, *134*, 4857. (d) Zhang, L. Y.; Xu, L. J.; Zhang, X.; Wang, J. Y.; Li, J.; Chen, Z. N. *Inorg. Chem.* **2013**, *52*, 5167. (e) Chen, B.; Xiang, S.; Qian, G. *Acc. Chem. Res.* **2010**, *43*, 1115. (f) Peng, P.; Li, F. F.; Neti, V.; Metta-Magana, A. J.; Echegoyen, L. *Angew. Chem., Int. Ed.* **2014**, *53*, 160. (g) Chen, L.; Jiang, F.; Lin, Z.; Zhou, Y.; Yue, C.; Hong, M. *J. Am. Chem. Soc.* **2005**, *127*, 8588. (h) Zeng, M. H.; Yao, M. X.; Liang, H.; Zhang, W. X.; Chen, X. M. *Angew. Chem., Int. Ed.* **2007**, *46*, 1832. (i) Padial, N. M.; Procopio, E. Q.; Montoro, C.; Lopez, E.; Oltra, J. E.; Colombo, V.; Maspero, A.; Masciocchi, N.; Galli, S.; Senkovska, I.; Kaskel, S.; Barea, E.; Navarro, J. A. R. *Angew. Chem., Int. Ed.* **2013**, *52*, 8290. (j) Liu, Q. K.; Ma, J. P.; Dong, Y. B. *J. Am. Chem. Soc.* **2010**, *132*, 7005. (k) Das, A.; Li, T.; Nobusada, K.; Zeng, C. J.; Rosi, N. L.; Jin, R. C. *J. Am. Chem. Soc.* **2013**, *135*, 18264. (l) Evangelisti, F.; Guttinger, R.; More, R.; Luber, S.; Patzke, G. R. *J. Am. Chem. Soc.* **2013**, *135*, 18734. (m) Xuan, W. M.; Zhang, M. N.; Liu, Y.; Chen, Z. J.; Cui, Y. *J. Am. Chem. Soc.* **2012**, *134*, 6904. (n) Zhao, X. L.; Liu, F. L.; Zhang, L. L.; Sun, D.; Wang, R. M.; Ju, Z. F.; Yuan, D. Q.; Sun, D. F. *Chem.—Eur. J.* **2014**, *20*, 649. (o) Ma, H. Q.; Sun, D.; Zhang, L. L.; Wang, R. M.; Blatov, V. A.; Guo, J.; Sun, D. F. *Inorg. Chem.* **2013**, *52*, 10732.

(2) (a) Hu, Z. C.; Pramanik, S.; Tan, K.; Zheng, C.; Liu, W.; Zhang, X.; Chabal, Y. J.; Li, J. *Cryst. Growth Des.* **2013**, *13*, 4204. (b) Tian, D.; Li, Y.; Chen, R. Y.; Chang, Z.; Wang, G. Y.; Bu, X. H. *J. Mater. Chem. A* **2014**, *2*, 1465. (c) O'Keeffe, M.; Yaghi, O. M. *Chem. Rev.* **2012**, *112*, 675. (d) Talin, A. A.; Centrone, A.; Ford, A. C.; Foster, M. E.; Stavila, V.; Haney, P.; Kinney, R. A.; Szalai, V.; El Gabaly, F.; Yoon, H. P.; Leonard, F.; Allendorf, M. D. *Science* **2014**, *343*, 66. (e) Nunez, A. J.; Chang, M. S.; Ibarra, I. A.; Humphrey, S. M. *Inorg. Chem.* **2014**, *53*, 282. (f) Yuan, D. Q.; Zhao, D.; Timmons, D. J.; Zhou, H. C. *Chem. Sci.* **2011**, *2*, 103. (g) Bi, Y. F.; Wang, X. T.; Liao, W. P.; Wang, X. F.; Wang, X. W.; Zhang, H. J.; Gao, S. *J. Am. Chem. Soc.* **2009**, *131*, 11650. (h) Zhou, X. P.; Liu, J.; Zhan, S. Z.; Yang, J. R.; Li, D.; Ng, K. M.; Sun, R. W. Y.; Che, C. M. *J. Am. Chem. Soc.* **2012**, *134*, 8042. (i) Zhou, X. P.; Li, M.; Liu, J.; Li, D. *J. Am. Chem. Soc.* **2012**, *134*, 67.

(3) (a) Li, B.; Wei, R. J.; Tao, J.; Huang, R. B.; Zheng, L. S.; Zheng, Z. P. *J. Am. Chem. Soc.* **2010**, *132*, 1558. (b) Fang, S. M.; Zhang, Q.; Hu, M.; Sanudo, E. C.; Du, M.; Liu, C. S. *Inorg. Chem.* **2010**, *49*, 9617. (c) Li, C.-P.; Du, M. *Chem. Commun.* **2011**, *47*, 5958. (d) Sun, D.; Li, Y.-H.; Hao, H.-J.; Liu, F.-J.; Wen, Y.-M.; Huang, R.-B.; Zheng, L.-S. *Cryst. Growth Des.* **2011**, *11*, 3323. (e) Sun, D.; Wei, Z. H.; Yang, C. F.; Wang, D. F.; Zhang, N.; Huang, R. B.; Zheng, L. S. *CrystEngComm* **2011**, *13*, 1591. (f) Lee, S. Y.; Jung, J. H.; Vittal, J. J.; Lee, S. S. *Cryst. Growth Des.* **2010**, *10*, 1033. (g) Deng, D. S.; Liu, L. L.; Ji, B. M.; Yin, G. J.; Du, C. X. *Cryst. Growth Des* **2012**, *12*, 5338. (h) Du, L. Y.; Shi, W. J.; Hou, L.; Wang, Y. Y.; Shi, Q. Z.; Zhu, Z. H. *Inorg. Chem.* **2013**, *52*, 14018. (i) Yin, Y. Y.; Ma, J. G.; Niu, Z.; Cao, X. C.; Shi, W.; Cheng, P. *Inorg. Chem.* **2012**, *51*, 4784.

(4) (a) Bury, W.; Fairen-Jimenez, D.; Lalonde, M. B.; Snurr, R. Q.; Farha, O. K.; Hupp, J. T. *Chem. Mater.* **2013**, *25*, 739. (b) Yaghi, O. M. *Nat. Mater.* **2007**, *6*, 92. (c) Lee, J. Y.; Kim, H. J.; Park, C. S.; Sim, W.; Lee, S. S. *Chem.—Eur. J.* **2009**, *15*, 8989. (d) Maji, T. K.; Matsuda, R.; Kitagawa, S. *Nat. Mater.* **2007**, *6*, 142. (e) Kitagawa, S.; Kitaura, R.; Noro, S. *Angew. Chem., Int. Ed.* **2004**, *43*, 2334. (f) Aromi, G.; Berzal, P. C.; Gamez, P.; Roubeau, O.; Kooijman, H.; Spek, A. L.; Driessen, W. L.; Reedijk, J. *Angew. Chem., Int. Ed.* **2001**, *40*, 3444. (g) Bi, W. H.; Cao, R.; Sun, D. F.; Yuan, D. Q.; Li, X.; Wang, Y. Q.; Li, X. J.; Hong, M. C. *Chem. Commun.* **2004**, 2104. (h) Qiu, W.; Perman, J. A.; Wojtas, L.; Eddaoudi, M.; Zaworotko, M. J. *Chem. Commun.* **2010**, *46*, 8734. (i) Sun, D.; Yan, Z.-H.; Liu, M.; Xie, H.; Yuan, S.; Lu, H.; Feng, S.; Sun, D. *Cryst. Growth Des* **2012**, *12*, 2902.

(5) (a) He, J.; Yin, Y.-G.; Wu, T.; Li, D.; Huang, X.-C. *Chem. Commun.* **2006**, 2845. (b) Boldog, I.; Daran, J.-C.; Chernega, A. N.; Rusanov, E. B.; Krautscheid, H.; Domasevitch, K. V. *Cryst. Growth Des* **2009**, *9*, 2895. (c) He, J.; Zhang, J.-X.; Tan, G.-P.; Yin, Y.-G.; Zhang, D.; Hu, M.-H. *Cryst. Growth Des* **2007**, *7*, 1508. (d) Boldog, I.; Rusanov, E. B.; Chernega, A. N.; Sieler, J.; Domasevitch, K. V. *Angew. Chem., Int. Ed.* **2001**, *40*, 3435. (e) Tabacaru, A.; Pettinari, C.; Timokhin, I.; Marchetti, F.; Carrasco-Marin, F.; Jose Maldonado-Hodar, F.; Galli, S.; Masciocchi, N. *Cryst. Growth Des* **2013**, *13*, 3087. (f) Xie, Y.-M.; Liu, J.-H.; Wu, X.-Y.; Zhao, Z.-G.; Zhang, Q.-S.; Wang, F.; Chen, S.-C.; Lu, C.-Z. *Cryst. Growth Des* **2008**, *8*, 3914. (g) Sun, Y.-Q.; Deng, S.; Liu, Q.; Ge, S.-Z.; Chen, Y.-P. *Dalton Trans.* **2013**, *42*,

10503. (h) Kara, H.; Adams, C. J.; Schwarz, B.; Orpen, A. G. *CrystEngComm* **2011**, *13*, 5082. (i) Zhang, J.-P.; Kitagawa, S. *J. Am. Chem. Soc.* **2008**, *130*, 907. (j) Boldog, I.; Rusanov, E. B.; Sieler, J.; Domasevitch, K. V. *New J. Chem.* **2004**, *28*, 756.

(6) (a) Xie, Y. P.; Mak, T. C. W. *J. Am. Chem. Soc.* **2011**, *133*, 3760. (b) Zhao, L.; Mak, T. C. W. *Inorg. Chem.* **2009**, *48*, 6480. (c) Zang, S. Q.; Mak, T. C. W. *Inorg. Chem.* **2008**, *47*, 7094. (d) Li, G.; Lei, Z.; Wang, Q.-M. *J. Am. Chem. Soc.* **2010**, *132*, 17678. (e) Jia, J.-H.; Wang, Q.-M. *J. Am. Chem. Soc.* **2009**, *131*, 16634.

(7) (a) Hsiao, H.-L.; Wu, C.-J.; Hsu, W.; Yeh, C.-W.; Xie, M.-Y.; Huang, W.-J.; Chen, J.-D. *CrystEngComm* **2012**, *14*, 8143. (b) Cheng, P.-C.; Yeh, C.-W.; Hsu, W.; Chen, T.-R.; Wang, H.-W.; Chen, J.-D.; Wang, J.-C. *Cryst. Growth Des* **2012**, *12*, 943. (c) Baum, G.; Constable, E. C.; Fenske, D.; Kulke, T. *Chem. Commun.* **1997**, 2043. (d) Schottel, B. L.; Chifotides, H. T.; Shatruk, M.; Chouai, A.; Perez, L. M.; Bacsa, J.; Dunbar, K. R. *J. Am. Chem. Soc.* **2006**, *128*, 5895. (e) Schottel, B. L.; Bacsa, J.; Dunbar, K. R. *Chem. Commun.* **2005**, 46. (f) Anson, C.; Eichhoefer, A.; Issac, I.; Fenske, D.; Fuhr, O.; Sevillano, P.; Persau, C.; Stalke, D.; Zhang, J. *Angew. Chem., Int. Ed.* **2008**, *47*, 1326. (g) Wang, M.-S.; Guo, S.-P.; Li, Y.; Cai, L.-Z.; Zou, J.-P.; Xu, G.; Zhou, W.-W.; Zheng, F.-K.; Guo, G.-C. *J. Am. Chem. Soc.* **2009**, *131*, 13572. (h) Hong, M. C.; Zhao, Y. J.; Su, W. P.; Cao, R.; Fujita, M.; Zhou, Z. Y.; Chan, A. S. C. *Angew. Chem., Int. Ed.* **2000**, *39*, 2468.

(8) (a) Yang, J.; Ma, J.-F.; Liu, Y.-Y.; Li, S.-L.; Zheng, G.-L. *Eur. J. Inorg. Chem.* **2005**, 2174. (b) Liu, Y.-Y.; Ma, J.-F.; Yang, J.; Su, Z.-M. *Inorg. Chem.* **2007**, *46*, 3027. (c) Ma, J.-F.; Yang, J.; Zheng, G.- L.; Li, L.; Liu, J.-F. *Inorg. Chem.* **2003**, *42*, 7531. (d) Li, F.-F.; Ma, J.-F.; Song, S.-Y.; Yang, J.; Liu, Y.-Y.; Su, Z.-M. *Inorg. Chem.* **2005**, *44*, 9374.

(9) (a) Fan, J.; Gan, L.; Kawaguchi, H.; Sun, W. Y.; Yu, K. B.; Tang, W. X. *Chem.—Eur. J.* **2003**, *9*, 3965. (b) Su, Z.; Fan, J.; Okamura, T.; Sun, W. Y.; Ueyama, N. *Cryst. Growth Des.* **2010**, *10*, 3515. (c) Xu, J.; Pan, Z. R.; Wang, T. W.; Li, Y. Z.; Guo, Z. J.; Batten, S. R.; Zheng, H. G. *CrystEngComm* **2010**, *12*, 612. (d) Wang, X. F.; Lv, Y.; Okamura, T. A.; Kawaguchi, H.; Wu, G.; Sun, W. Y.; Ueyama, N. *Cryst. Growth Des.* **2007**, *7*, 1125. (e) Su, Z.; Chen, M. S.; Fan, J. A.; Chen, M.; Chen, S. S.; Luo, L.; Sun, W. Y. *CrystEngComm* **2010**, *12*, 2040. (f) Su, Z.; Song, Y.; Bai, Z. S.; Fan, J. A.; Liu, G. X.; Sun, W. Y. *CrystEngComm* **2010**, *12*, 4339.

(10) (a) Allen, F. H. *Acta Crystallogr., Sect. B: Struct. Sci.* **2002**, *58*, 380. (b) Cambridge Structure Database search, CSD Version 5.28 (November 2006) with 20 updates (January 2007−May 2013).

(11) (a) Zhang, J.-P.; Horike, S.; Kitagawa, S. *Angew. Chem., Int. Ed.* **2007**, *46*, 889. (b) Domasevitch, K. V.; Boldog, I.; Rusanov, E. B.; Hunger, J.; Blaurock, S.; Schroder, M.; Sieler, J. *Z. Anorg. Allg. Chem.* **2005**, *631*, 1095. (c) Boldog, I.; Rusanov, E. B.; Chernega, A. N.; Sieler, J.; Domasevitch, K. V. *Polyhedron* **2001**, *20*, 887. (d) Xie, Y.-M.; Yu, R.-M.; Wu, X.-Y.; Wang, F.; Zhang, J.; Lu, C.-Z. *Cryst. Growth Des* **2011**, *11*, 4739. (e) Hunger, J.; Krautscheid, H.; Sieler, J. *Cryst. Growth Des* **2009**, *9*, 4613.

(12) (a) Sun, D.; Liu, F.-J.; Huang, R.-B.; Zheng, L.-S. *Inorg. Chem.* **2011**, *50*, 12393. (b) Sun, D.; Zhang, L.; Yan, Z.; Sun, D. F. *Chem—Asian J.* **2012**, *7*, 1558. (c) Sun, D.; Wang, H.; Lu, H.-F.; Feng, S.-Y.; Zhang, Z.-W.; Sun, G.-X.; Sun, D.-F. *Dalton Trans.* **2013**, *42*, 6281. (d) Yuan, S.; Deng, Y.-K.; Wang, X.-P.; Sun, D. *New J. Chem.* **2013**, *37*, 2973. (e) Sun, D.; Yan, Z.-H.; Liu, M.; Xie, H.; Yuan, S.; Lu, H.; Feng, S.; Sun, D. F. *Cryst. Growth Des* **2012**, *12*, 2902.

(13) Bruker. *SMART*, *SAINT*, and *SADABS*. Bruker AXS Inc.: Madison, Wisconsin, USA, 1998.

(14) Sheldrick, G. M. *SHELXS-97, Program for X-ray Crystal Structure Determination*; University of Gottingen: Germany, 1997.

(15) Sheldrick, G. M. *SHELXL-97, Program for X-ray Crystal Structure Refinement*; University of Gottingen: Germany, 1997.

(16) Blatov, V. A. *Struct. Chem.* **2012**, *23*, 955. TOPOS software is available for download at http://www.topos.samsu.ru.

(17) (a) Dong, Y. B.; Zhao, X.; Tang, B.; Wang, H. Y.; Huang, R. Q.; Smith, M. D.; zur Loye, H. C. *Chem. Commun.* **2004**, 220. (b) Dong, Y. B.; Geng, Y.; Ma, J. P.; Huang, R. Q. *Inorg. Chem.* **2005**, *44*, 1693. (c) Dong, Y. B.; Wang, P.; Huang, R. Q. *Inorg. Chem.* **2004**, *43*, 4727. (d) Hou, G.-G.; Wu, Y.; Ma, J.-P.; Dong, Y.-B. *CrystEngComm* **2011**, *13*, 6850. (e) Wang, X.; Huang, J.; Xiang, S.; Liu, Y.; Zhang, J.; Eichhoefer, A.; Fenske, D.; Bai, S.; Su, C.-Y. *Chem. Commun.* **2011**, *47*, 3849.

(18) (a) Chen, C. L.; Su, C. Y.; Cai, Y. P.; Zhang, H. X.; Xu, A. W.; Kang, B. S.; zur Loye, H. C. *Inorg. Chem.* **2003**, *42*, 3738. (b) Chen, C. L.; Tan, H. Y.; Yao, J. H.; Wan, Y. Q.; Su, C. Y. *Inorg. Chem.* **2005**, *44*, 8510. (c) Li, X.-P.; Zhang, J.-Y.; Pan, M.; Zheng, S.-R.; Liu, Y.; Su, C.-Y. *Inorg. Chem.* **2007**, *46*, 4617. (d) Wu, H.; Yang, J.; Su, Z.-M.; Batten, S. R.; Ma, J.-F. *J. Am. Chem. Soc.* **2011**, *133*, 11406. (e) Yin, P. X.; Cheng, J. K.; Li, Z. J.; Zhang, L.; Qin, Y. Y.; Zhang, J.; Yao, Y. G. *Inorg. Chem.* **2009**, *48*, 10859.

(19) Yang, L.; Powell, D. R.; Houser, R. P. *Dalton Trans.* **2007**, 955.

(20) (a) Majeed, Z.; Mondal, K. C.; Kostakis, G. E.; Lan, Y.; Anson, C. E.; Powell, A. K. *Chem. Commun.* **2010**, *46*, 2551. (b) Zhang, J.; Chen, S.; Zingiryan, A.; Bu, X. *J. Am. Chem. Soc.* **2008**, *130*, 17246.

(21) Blatov, V. A.; Carlucci, L.; Ciani, G.; Proserpio, D. M. *CrystEngComm* **2004**, *6*, 377.

(22) (a) Bondi, A. *J. Phys. Chem.* **1964**, *68*, 441. (b) Pyykko, P. *Chem. Rev.* **1997**, *97*, 597. (c) Zhang, J.-P.; Wang, Y.-B.; Huang, X.-C.; Lin, Y.-Y.; Chen, X.-M. *Chem.—Eur. J.* **2005**, *11*, 552. (d) Ray, L.; Shaikh, M. M.; Ghosh, P. *Inorg. Chem.* **2008**, *47*, 230. (e) Che, C.-M.; Tse, M.-C.; Chan, M. C. W.; Cheung, K.-K.; Phillips, D. L.; Leung, K.-H. *J. Am. Chem. Soc.* **2000**, *122*, 2464.

(23) (a) See the website: http://rcsr.anu.edu.au. (b) Xie, Y. M.; Zhao, Z. G.; Wu, X. Y.; Zhang, Q. S.; Chen, L. J.; Wang, F.; Chen, S. C.; Lu, C. Z. *J. Solid State Chem.* **2008**, *181*, 3322.

(24) (a) Sun, D.; Xu, Q.-J.; Ma, C.-Y.; Zhang, N.; Huang, R.-B.; Zheng, L.-S. *CrystEngComm* **2010**, *12*, 4161. (b) Sun, D.; Yuan, S.; Wang, H.; Lu, H.-F.; Feng, S.-Y.; Sun, D.-F. *Chem. Commun.* **2013**, *49*, 6152.

(25) (a) Etter, M. C. *Acc. Chem. Res.* **1990**, *23*, 120. (b) Bernstein, J.; Davis, R. E.; Shimoni, L.; Chang, N.-L. *Angew. Chem., Int. Ed., Engl.* **1995**, *34*, 1555.

(26) Eisenberg, D.; Kauzmann, W. *The Structure and Properties of Water*; Oxford University Press: Oxford, U.K., 1969.

(27) Barbour, L. J.; Orr, G. W.; Atwood, J. L. *Nature* **1998**, *393*, 671.

(28) Jun, H.; Zhang, J.-X.; Tan, G.-P.; Yin, Y.-G.; Zhang, D.; Hu, M.-H. *Cryst. Growth Des.* **2007**, *7*, 1508.

(29) (a) Pan, Z. R.; Song, Y.; Jiao, Y.; Fang, Z. J.; Li, Y. Z.; Zheng, H. G. *Inorg. Chem.* **2008**, *47*, 5162. (b) Li, F. F.; Ma, J. F.; Song, S. Y.; Yang, J.; Liu, Y. Y.; Su, Z. M. *Inorg. Chem.* **2005**, *44*, 9374. (c) Cui, Y.; Yue, Y.; Qian, G.; Chen, B. *Chem. Rev.* **2012**, *112*, 1126.

(30) Zhu, Q.; Shen, C.; Tan, C.; Sheng, T.; Hu, S.; Wu, X. *Chem. Commun.* **2012**, *48*, 531.